DOI: 10.61782/fa.2025.0247

FORUM ACUSTICUM
EURONOISE 2025

COMPRESSED SENSING FOR DATA ACQUISITION IN IN-AIR IMAGING SONAR SENSORS

Ahmad Sharifa [1,2] **Jan Steckel** [1,2*]
[1] CoSys-lab - Faculty of Applied Engineering, University of Antwerp, Belgium.
[2] Flanders Make Strategic Research Centre, Lommel, Belgium.

ABSTRACT

This paper aims to apply compressed sensing to in-air ultrasound imaging sensors to enhance efficiency in data acquisition and signal processing. In most state of the art sonar sensor systems, the utilized beamforming techniques for array signal processing require each transducer element in a sensor array to be sampled at a rate exceeding the Nyquist criterion. This results in a substantial amount of data to be received, stored and processed. To address this challenge, this research uses the eRTIS, an Embedded Real-Time Imaging Sonar with enhanced real-time imaging capabilities as a case study, focusing on data acquisition and signal processing. Consequently, processing such a high volume of data can strain computational resources, necessitate significant storage capacity, and increase the system's power consumption. Therefore, this paper investigates the application of data-reduction strategies such as compressive sensing which offers the advantage of reducing the amount of data needed without compromising quality, to make eRTIS more efficient, high-performance, and manageable. In this respect, L1 minimization, OMP and SBL algorithms were selected for their demonstrated efficacy in handling sparse data and used to reconstruct the randomly-sampled signals. Furthermore, a MATLAB simulation model was developed to extract the results, which were analyzed extensively.

Keywords: *compressed sensing, in-air ultrasound imaging, data acquisition, signal processing, data reduction strategies.*

[*] ***Corresponding author***: *Jan.Steckel@uantwerpen.be.*

1. INTRODUCTION

We are interested in investigating the compressed sensing paradigm in the context of in-air 3D ultrasonic imaging. This technique is widely used in various fields, including in-air 3D object detection, industrial inspection, monitoring of harsh environment, autonomous robotic navigation, localization and mapping systems based on ultrasound waves.

The eRTIS is an Embedded Real-Time Imaging Sensor developed by the research group in the CoSys lab, University of Antwerp, Belgium [1]. It signifies a major advancement in ultrasonic technology by advancing 3D object detection in-air. Moreover, modern sonar systems tend to use MEMS microphone arrays [2]. In many cases, these systems involve phased array configurations with many receive elements [3]. However, traditional time-domain beamforming techniques require each transducer element in a sensor array to be sampled at a rate exceeding the Nyquist criterion. This generates substantial amounts of data, which must be received, stored and processed, posing considerable challenges in terms of computational resources, storage capacity and power consumption.

This paper aims to optimize the signal processing flow in eRTIS by reducing the data load and computational complexity associated with 3D image processing, which is crucial for enhancing performance and boosting the efficiency of acoustic imaging systems. Moreover, the focus is on implementing data reduction strategies using the compressed sensing method to acquire and reconstruct microphone signals by exploiting their sparsity. Furthermore, data acquisition is an essential step in the processing pipeline of an in-Air Imaging Sonar Sensor. However, several data acquisition techniques that have been proposed suffer from high processing time, hardware cost and computational complexity [4].

Compressed sensing (CS) is a promising signal processing technique which enables the acquisition and reconstruction of sparse and compressible signals from severely under-sampled measurements than traditionally required by the Nyquist-Shannon sampling theorem. This approach exploits the sparsity of signals in a specific domain, allowing for efficient data acquisition and significant reductions in sampling rates [5]. Besides, CS achieves this by finding solutions to under-determined linear systems, making it an emerging technique in signal and image processing for data compression and recovery. Theoretically, it has been guaranteed that recovery of the information is possible if the original signal and the measurement matrix satisfy certain mathematical conditions [6].

Compressed sensing is a widely used data reduction strategy that reduces computational complexity while maintaining system performance. This approach's effectivity depends on different parameters including sparsity of the signal, measurement matrix, reconstruction algorithm, noise levels, coherence of the measurement matrix, sampling rate. Thus, the quantity of measurements required to reconstruct a signal is determined by its sparsity instead of its bandwidth [7]. In this paper, three reconstruction algorithms were investigated and compared in performance.

Compressed sensing (CS) has found applications in various domains due to its ability to acquire and reconstruct signals efficiently. In medical imaging, it is extensively used in magnetic resonance imaging (MRI) to reduce scan times while maintaining image quality [8]. Similarly, in astronomy, it helps process astronomical data, enabling the reconstruction of high-resolution images from fewer measurements [9]. CS is also applied in wireless communications for channel estimation and spectrum sensing, improving the efficiency of wireless networks [10]. Additionally, in geophysics, it aids in reconstructing subsurface images from seismic data, which is crucial for oil and gas exploration [11]. Specifically, in the context of 3D sonar, CS is valuable for synthetic aperture sonar (SAS) imaging, allowing the reconstruction of high-resolution 3D images from fewer measurements, benefiting underwater exploration and mapping [12]. Furthermore, it has been effectively utilized in 3D ultrasonic imaging to enhance the detection and localization of air leaks in pressurized air systems. Steckel and Peremans demonstrated this approach by employing a random, sparse array of microphones and CS algorithms to accurately localize air leaks in two dimensions, thereby improving the precision and reliability of ultrasonic imaging systems [13].

Prior to compressed sensing (CS), various data reduction strategies were used in ultrasonic images to manage processing time. Hardware costs and computational complexity were handled by interpolating sub-frequency bands using Discrete Wavelet Transform (DWT), which selectively decomposes the ultrasonic signal into different frequency bands. Consequently, data volume can be reduced by eliminating some sub-bands [14]. Full Matrix Capture (FMC) is a data acquisition method used in ultrasonic imaging to capture every possible transmit-receive combination for a given ultrasonic phased array transducer. While FMC generates large data volumes, post-acquisition strategies are required to handle and process this data effectively [15]. Thus, data is selectively sampled in the lateral axial direction to reduce the number of active access elements and amount of data collected [16]. In comparison, compressed sensing is superior to these methods; taking advantage of signal sparsity to reconstruct high-quality images from significantly fewer samples. This results in faster data acquisition, reducing hardware requirements and complexity in calculations [17].

The rest of this paper is structured as follows: firstly, an overview of the conventional signal processing flow in eRTIS is introduced. Building on this, the research focuses on optimizing signal acquisition and digital processing algorithms in the CoSys-lab eRTIS sensor operating in harsh environments such as mining, agriculture, construction equipment and other similar scenarios where the optical techniques often fail. With the introduction of dense sensor arrays in ultrasound imaging, data transfer rate and data storage can become a bottleneck in system design. Secondly, we introduce compressed sensing to reduce the amount of sampled channel data. Consequently, we propose a new approach based on compressed sensing in data acquisition. In addition, compressed sensing provides a significant computational savings during on-chip implementation. Therefore, it is considered the most feasible technique to boost the performance. Thirdly, three sparse recovery algorithms are implemented, leveraging the sparsity of the signal received at each transducer element to reduce sensor complexity while maintaining imaging quality. Finally, the study's validation is demonstrated through a simulation model in MATLAB where proof-of-concept implementations are demonstrated.

2. CONVENTIONAL SIGNAL PROCESSING FLOW IN ERTIS:

The eRTIS system is an active airborne ultrasound sensing utilizes ping-based processing across multiple stages to achieve 3D imaging. A detailed overview of the processing pipeline of the eRTIS is shown in Figure (1) These steps collectively transform the raw acoustic data into high-resolution images that can be used for detailed analysis and interpretation.

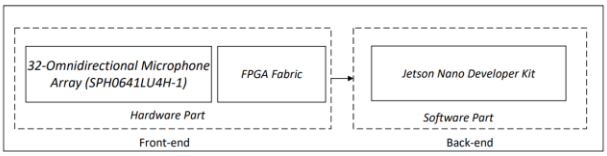

a) Architecture of embedded real time imaging sonar.

b) The CoSys-Lab eRTIS sensor [8] in a custom enclosure.

Figure 1. a) A schematic overview of the components used in this paper. The eRTIS front-end is by default connected to the eRTIS backend, which will handle the microphone data. A USB connection between the eRTIS backend and the Jetson Nano is used to transfer data to Jetson Nano's memory, where the measurements can be stored. b) The CoSys-Lab eRTIS sensor [1] in a custom enclosure.

In the front-end of the eRTIS, the Sens Comp 7000 transducer [18] emits a broadband ultrasonic chirp ranging from 20 kHz to 80 kHz, which reflects off objects in the field of view (FOV) environment. Subsequently, each MEMS microphone in the 32-Omnidirectional microphone array simultaneously and individually receives the reflected echoes. Due to the broad distribution of acoustic energy in the frontal hemisphere and the near omnidirectional nature of the microphones, the sensor's field-of-view covers the frontal hemisphere [19][20].
These reflected signals are modulated using a pulse density modulator (PDM) integrated into the MEMS microphone. Afterward, these Mono PDM signals $x_1[n] \dots x_{32}[n]$ are demodulated using a decimation stage that converts one-bit PDM microphone signals to 16-bit PCM format $\acute{x}_1[n] \dots \acute{x}_{32}[n]$, which in turn serves as the input to the back-end of the eRTIS.

It is important to highlight that the microphone signals are require at each transducer element in a sensor array to be sampled at a rate higher than the Nyquist criterion, resulting in an extensive amount of data to be received, stored, and processed. Therefore, sampling 32 elements of a microphone array at 4.5 MHz, while respecting the Nyquist criterion, results in a data rate of 144 Mbps. Alongside the decimation stage performed in the Field-Programmable Gate Array (FPGA) at the front-end, these signals are processed using a bandpass filter to limit the signals' frequency to the desired range. The decimation stage utilizes an IIR 6th order Butterworth low pass filter with a cutoff frequency of 100kHz. Once filtered a decimation of factor 10 is used, which effectively gets us the data sampled at 450kHz The filtered signals $\tilde{x}_1[n] \dots \tilde{x}_{32}[n]$.

In the back-end of the eRTIS, the initial signal processing step involves a matched filter that enhances the signal-to-noise ratio and compresses the emitted pulse into its auto-correlation function, resulting in the pulse compressed signal (see Figure 2).

$$S_i^{MF}[k] = \mathcal{F}^{-1}\{\, S_i^M[j\omega].S_b^*[j\omega]\} \qquad (1)$$

In Eqn. (1), $\mathcal{F}^{-1}$ represents the inverse Discrete Fourier Transform (DFT) applied to the discrete Fourier transforms of the signal from the i_th microphone channel, $S_i^M[j\omega]$, and the complex conjugate of the Fourier transform of the emitted signal $S_b^*[j\omega]$. The subsequent step involves the beamformer, which functions as an acoustic lens directed towards a specific angle ψ in the frontal hemisphere. Here, $\psi = [\theta\ \varphi]^T$, where θ is the azimuth angle and φ is the elevation angle.

The matched filter is designed to align with the shape of the transmitted ultrasound pulse, which is known a priori, and peaks when it detects the desired signal. This peak helps separate the wanted reflection from background noise. Moreover, the matched filter output is a compressed

version of the original signal, which reduces its duration. This compression makes it easier to distinguish between closely spaced reflectors, enhancing the signal-to-noise ratio (SNR) and improving resolution.

The microphone signals are then combined with a conventional delay-and-sum (DAS) beamforming algorithm that processes the digital signals to introduce directionality in the reception stage. Consequently, the array is digitally steered in predefined desired directions of arrival in post processing technique, rotating in the horizontal plane ranging from -90° to 90° in steps of 2°.

Eqn. (2) describes how the beamformer operates. Currently, a delay-and-sum (or time-domain Bartlett) beamformer is used due to its simplicity and robustness against calibration errors. However, more advanced beamformers can be implemented to achieve better peak-to-sidelobe ratios in the imaging point spread function [21]. It is important to note that most data-dependent beamformers require multiple data snapshots, which may not always be feasible in robotic applications where the sensor moves quickly through the environment relative to the sonar sensor's sampling rate of 10-15Hz. To address the limitations of data-dependent beamformers, sparsity-based segmentation techniques of the acoustic images can be used to improve object localization accuracy, as previously demonstrated in [22]. For the time-domain Bartlett beamformer, time-delays $\tau_i(\psi)$ are added to each channel to compensate for the angle-dependent differences in time-of-arrival caused by the array's geometry.

$$S_{\psi}^{BF}[k] = \sum_{i=1}^{32} \omega_i .\ S_i^{MF}[k + \tau_i(\psi)] \quad (2)$$

Where ω_i is a weight assigned to the channels are selected using a Gaussian window over the array aperture to minimize sidelobe levels in the point spread function (PSF) and $\tau_i(\psi)$ are the direction dependent delays given by the Bartlett Beamformer [21].

The final step involves performing envelope detection for each direction ψ, where the envelope of the beamformed signal is calculated by full-wave rectification and low-pass filtering.

$$S_{\psi}^{EN}[k] = \left| S_{\psi}^{BF}[k] \right| \times \mathrm{h_{1p}}[k] \quad (3)$$

Where $\mathrm{h_{1p}}$ is a low-pass filter (2nd order Butterworth filter, cutoff frequency = 1kHz). The signal $S_{\psi}^{EN}[k]$ contains the envelope of the beamformed signal in direction ψ.

This process generates a collection of range-energy profiles $(S_{(\theta\,\varphi)}^{EN}[k])$. These range-energy profiles from the desired directions are then combined into a single image, referred to as the Energyscape (ES) of the environment [23].

Finally, envelope detection stage extracts the energy-profile in function of range and several of these range-energy profiles are combined to form an acoustic image, called the Energyscape. That is to say, this stage is performed to represent the reflector distribution for each particular direction, with the time axis representing the range for that direction. These stages are all necessary to create acoustic images, which are 2D or 3D images that provide the intensity, range, and direction for each detected reflector.

$$E(k,\psi) = \begin{bmatrix} S_{(\theta 1,\varphi 1)}^{EN}[k] & (S_{(\theta 2,\varphi 1)}^{EN}[k] & \cdots & (S_{(\theta n,\varphi 1)}^{EN}[k] \\ S_{(\theta 1,\varphi 2)}^{EN}[k] & S_{(\theta 2,\varphi 2)}^{EN}[k] & & S_{(\theta n,\varphi 2)}^{EN}[k] \\ \vdots & \ddots & & \vdots \\ S_{(\theta 1,\varphi m)}^{EN}[k] & S_{(\theta 2,\varphi m)}^{EN}[k] & \cdots & S_{(\theta n,\varphi m)}^{EN}[k] \end{bmatrix} \quad (3)$$

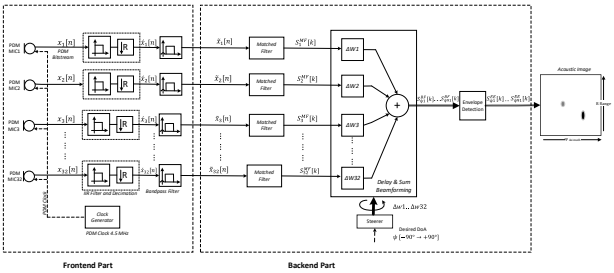

Figure 2. Classical diagram of the digital signal processing steps in eRTIS, the process begin with the raw microphone signals $\mathrm{x_1}[n] \ldots \mathrm{x_{32}}[n]$, which are pulse density modulated (PDM) signals oversampled at 4.5 MHz. These signals then are then demodulated to obtain the full ultrasonic signals of the N channels $\acute{x}_1[n] \ldots \acute{x}_{32}[n]$, represented as 16-bit PCM data sampled at 450 KHz, filtered by IIR and decimated by a factor of 10. The filtered signals $\tilde{x}_1[n] \ldots \tilde{x}_{32}[n]$. are within the target frequency range of 20 KHz to 80 KHz. Next, in pre-processing stage, the discrete time Fourier transform is applied to obtain $y_1[n] \ldots y_{32}[n]$. A matched filter is then used to find the actual reflections of the emitted signal, resulting in $S_1^{MF}[k] \ldots S_{32}^{MF}[k]$. Delay-and-sum beamforming creates a spatial filter for every direction of interest, producing $S_{\psi 1}^{BF}[k] \ldots S_{\psi 91}^{BF}[k]$. Finally, envelope detection is used to clean up the spatial image, yielding the Energyscape signals $S_{\psi 1}^{EE}[k] \ldots S_{\psi 91}^{EE}[k]$,

which correspond directly to the finished acoustic image.

3. COMPRESSIVE SENSING IN IN-AIR 3D SONAR SYSTEM:

In a MEMS microphone, a digital transducer converts the acoustic signal to an electrical signal, then an internal sigma-delta modulator converts the electrical analogue signal to a digital pulse density modulated (PDM) bitstream with over sampling rate (OCR=10). For Ultrasonic applications, the PDM bitstream is delivered at a sampling rate typically in the 1MHz to 3MHz range, while the audio or baseband signal is supposed to be in the 20 Hz to 20 kHz range. The modulator's order depends on the vendor and they are generally 2nd or higher order. The modulator shapes the quantization noise at higher frequencies while the audio signal remains in the baseband range. This quantization noise shaping is performed by analogue feedback and oversampling stages within the modulator with the intention of increasing the signal-to-noise ratio (SNR) at baseband frequencies [24].

Pulse Density Modulation (PDM) signals themselves are not inherently sparse in the time domain because they are oversampled one-bit signals that represent the density of pulses corresponding to the amplitude of the original signal. Furthermore, one-bit data will cause high quantization noise, resulting in a flat spectrum that is not sparse. Only after low-pass filtering and decimation can the signal become sparse. Therefore, Pulse Coded Modulation (PCM) can exhibit sparsity in frequency domain or a transformed domain, depending on the nature of the original signal and the modulation process.

3.1 The theoretical fundamental of compressive sensing:

The traditional data acquisition techniques are based on a set of measurements sampled at the Nyquist rate by an Analog/Digital Converter (ADC), which can result in a very high processing time, hardware cost, and computational complexity [26]. The Nyquist-Shannon sampling theorem asserts that to accurately and uniquely reconstruct a signal, the sampling rate must be at least double the highest frequency in the signal. Moreover, this theorem remains valid; if a single unit of data in a white noise signal is missed, the original signal cannot be recovered [25]. This is because white noise is inherently non-sparse, as it includes all frequencies with equal intensity, making it impossible to represent with just a few non-zero coefficients. In contrast, ultrasonic signals in the eRTIS are not white noise. A particularly significant aspect of compressed sensing is the underlying matrix computation. A raw signal can be regarded as a vector x with numerous components. We assume that x can be represented as a linear combination of specific basis functions:

$$x = \psi c \tag{4}$$

This basis must be suited to a particular application. In the Eqn. (4) , ψ, is the discrete cosine transform. We also assume that most of the coefficients c are effectively zero, so that c is sparse. Therefore, x can be either exactly c-sparse in the time domain or approximately sparse in a transform domain, such as Fourier basis, Discrete Cosine transform and wavelet, etc.

An exactly c-sparse signal is defined as $\|x\|_0 = c$ whereas the approximately sparse signal $x = \psi\phi$ is defined as $\|\phi\|_0 = c$. This implies that most of signal information is contained in the c coefficients of the signal x_s transformed representation. We represent φ_p norm of a vector x as:

$$\varphi_p = (\sum_{i=1}^{N} |x_i|^p)^{1/p} \tag{5}$$

In this paper, we refer to y as a few random samples of x, so ϕ is a subset of the rows of the identity operator. But more complicated sampling operators are possible. To reconstruct the signal, we must try to recover the coefficients by solving the following equation:

$$y = Ax, \text{ where } A = \psi\phi \tag{6}$$

Once we have the coefficients, we can recover the signal itself by inverse transform domain. Since this is a compression, A is rectangular fat matrix, with many more columns than rows. Computing the coefficients x involves solving an underdetermined system of simultaneous linear equations, $Ax = y$. In this situation, there are many more unknowns than equations. The key to the almost magical reconstruction process is to impose a nonlinear regularization involving the $\varphi_1$norm.

3.2-The compressed sensing for acquisition in the eRTIS:

The current time-domain beamforming techniques require the signal at each transducer-element to be sampled at a rate higher than the Nyquist criterion, resulting in an extensive amount of data to be received, stored and processed. For example, sampling 32 elements of a microphone array by 4.5MHz will end up by 144 Mbps.

As shown in Figure (3) and (4), compressive sensing involves two main processes: first part is sparse representation and measurement , and second parts is sparse signal recovery algorithm (SSR) [27]. Firstly, a measurement matrix called sensing matrix ϕ should be used to collect the information and simultaneously compress signals, which can be shown as the part associated with compressing and sampling with low-speed. Secondly, the recovery of signals after transmitting and storage should be accomplished by solving an optimization problem with effective algorithms.

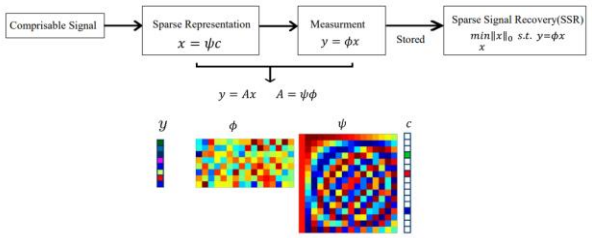

Figure 3. Compressive sensing processes has two primary components: compressive sampling (CS) and sparse signal recovery (SSR).

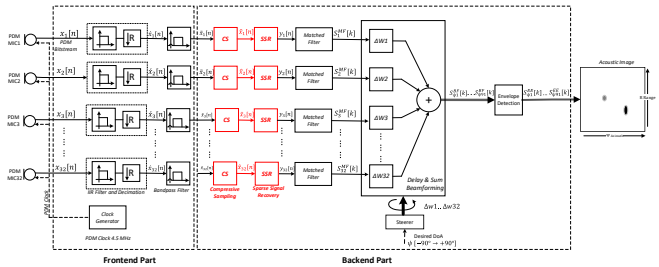

Figure 4. Signal processing of the eRTIS incorporates compressed sensing applied at the backend which comprises two primary components: compressed sampling (CS) and sparse signal recovery (SSR).

3.3- Spare Reconstruction Algorithms:

Compressive sensing relies on mathematical algorithms solving the problem of data reconstruction from a significantly reduced number of measurements by exploring the properties of sparsity and incoherence. Therefore, this concept includes optimization procedures aiming to provide the sparsest solution in a suitable representation domain. Moreover, to find the sparse solution for the underdetermined linear system, the φ_0 norm optimization problem should be solved. This is a non-deterministic polynomial-time hard (NP-hard) combinatorial search problem, which is a prohibitively expensive operation. However, φ_0-minimization does not have an efficient algorithm because the objective function is not convex. Therefore, an approximate solution has to be investigated.

There are two fundamental approaches for reconstructing from CS measurements: convex optimization and greedy search algorithms. If the measurement matrix obeys the restricted isometric property (RIP) with a sufficiently small constant and there is no measurement noise, it is possible to exactly recover signals from the measurement vector y using convex optimization [27]. In this paper, a standard Gaussian distributed sensing matrix will be used. The application of φ_1 norm minimization technique as recovery algorithm was firstly evaluated and then compared to two other competitive algorithms.

On the one hand, the sparse recovery approximation using conversion of φ_1 norm minimization to linear programming has been implemented on our eRTIS platform using MATLAB simulation. The number of measurements, M, sufficient for successful recovery via the L1 minimization is well known to be:

$$M = O(Klog(N / K)) \tag{7}$$

The implementation of the selected compressed sampling and the signal reconstruction algorithms was performed in MATLAB. The results were then compared with each other and presented in Figure (5) and 6). It is important to note that the implementation of the PDM to PCM conversion including filtering stage was performed using an FPGA in the front end. Therefore, the compressed sampling is done ultimately in the software at the backend. In the latest version of the eRTIS a Jetson Nano from Nvidia is used process the signals.

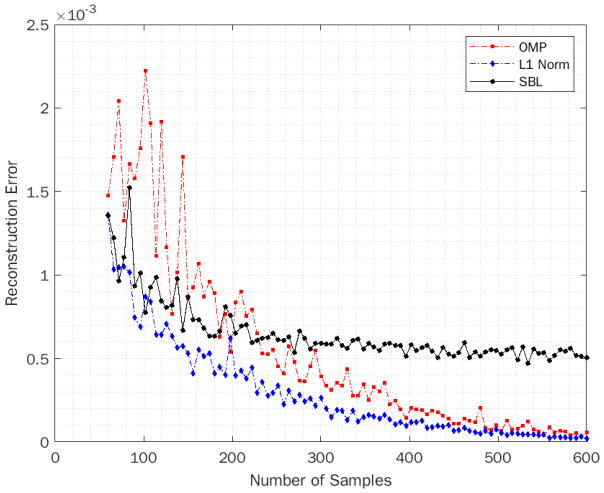

Figure 5. Reconstruction error versus the number of remaining samples after compression for L1 minimization, OMP, and SBL algorithms.

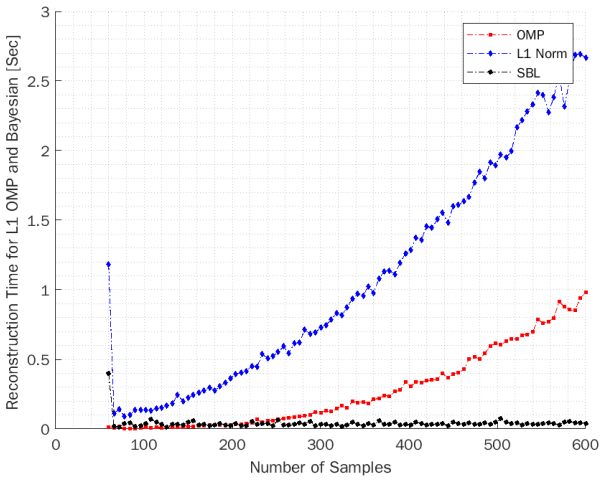

Figure 6. Reconstruction time versus the number of remaining samples after compression for L1 minimization, OMP, and SBL algorithms.

4. DISCUSSION AND CONCLUSION:

In this paper, we compared three sparse recovery algorithms from the convex relaxation, greedy, and Bayesian categories. We used two metrics: recovery error and recovery time. Figure (6) shows recovery time, which is a quantitative metric that assesses the duration required by each algorithm to accurately resolve the sparse recovery problem. The full dimensional signal has 12,500 samples. As shown in Figure (5), Bayesian techniques and Orthogonal Matching Pursuit show better performance in terms of recovery error which decreases to reach nearly 0% when the number of measurements exceeds 600 samples, which represents just 5% out of the full dimensional signal.

Greedy techniques are known for their speed, making them the fastest among the methods. This is evident from the very small reconstruction time in figure (6). On the other hand, convex relaxation techniques are very efficient in minimizing recovery errors, providing superior performance in this aspect. Bayesian techniques have a balance, offering both low recovery error and short recovery time, making them well-rounded in their performance. The ultrasound received signals in the eRTIS have a correlation structure. The reconstruction efficiency of the algorithms deteriorates if the correlation structure is ignored. This aspect has been ignored by most state-of-the-art algorithms.

Sparse Bayesian Learning (SBL) methods take advantage of the signal correlation structure to make significant improvements in reconstruction efficiency. It is reported in the literature [28] that the exploitation of the correlation structure with the sparsity of the non-sparse ultrasound signals may significantly increase the efficiency of reconstruction. It is demonstrated in Figure (6) that the SBL algorithms obtain the highest speed to reconstruct sparse signals.

Future work will involve the application of steerable compressed sensing. This technique allows for sparse scanning, eliminating the need to scan the field thoroughly. Instead, we can randomly scan the field for obstacles.

5. REFERENCES:

[1] R. Kerstens, D. Laurijssen, and J. Steckel, “eRTIS: A Fully Embedded Real Time 3D Imaging Sonar Sensor for Robotic Applications,” in *Proc. 2019 Int. Conf. Robot. Autom. (ICRA),* Montreal, QC, Canada, May 2019, pp. 1234-1240.

[2] D. Laurijssen, W. Daems, and J. Steckel, “HiRIS: An Airborne Sonar Sensor with a 1024 Channel Microphone Array for In-Air Acoustic Imaging, ” *IEEE Access*, vol. 12, pp. 12345-12356,Apr. 2024.

[3] C. Bahr, J. Smith, A. Johnson, and M. Lee, “Measurement of Phased Array Point Spread

Functions for use with Beamforming, " *Proceedings of the IEEE International Conference on Acoustics, Speech, and Signal Processing,*" (ICASSP), pp. 1234-1238, 2023.

[4] W. Jansen, D. Laurijssen, R. Kerstens, W. Daems, and J. Steckel, "In-Air Imaging Sonar Sensor Network with Real-Time Processing Using GPUs," *arXiv preprint arXiv:2208.10839*, 2022.

[5] R. Baeyens, J. Denil, J. Steckel, D. Laurijssen, and W. Daems, "Automated Firmware Generation for Compressive Sensing on Heterogeneous Hardware, " *Sensors*, vol. 22, no. 21, pp. 8147, 2022.

[6] Romberg, J. Compressive sensing by random convolution. *IEEE Transactions on Signal Processing*, 57(6), 2009-2021.

[7] E. Candes, J. Romberg, and T. Tao, "Stable Signal Recovery from Incomplete and Inaccurate Measurements, " Communications on Pure and Applied Mathematics, vol. 59, no. 8, pp. 1207-1223, Aug. 2006.

[8] M. Lustig, D. Donoho, and J. M. Pauly, "Sparse MRI: The application of compressed sensing for rapid MR imaging," *IEEE Signal Processing Magazine*, vol. 25, no. 2, pp. 72–82, 2007.

[9] J. Bobin, J.-L. Starck, J. Fadili, and Y. Moudden, "Sparsity and morphological diversity in blind source separation," *IEEE Transactions on Image Processing*, vol. 16, no. 11, pp. 2662–2674, 2008.

[10] R. Sankararajan, H. Rajendran, and A. N. Sukumaran, "Compressive Sensing for Wireless Communication: Challenges and Opportunities," *IEEE Xplore*, 2016. ISBN: 9788793379862.

[11] F. J. Herrmann, H. Wason, and T. T. Y. Lin, "Randomized sampling and sparsity: Getting more information from fewer samples," *Geophysics*, vol. 75, no. 6, pp. WB173–WB187, 2010.

[12] J. Steckel and H. Peremans, "Broadband 3-D sonar system using a sparse array for indoor navigation," IEEE Transactions on Robotics, vol. 29, no. 1, pp. 161–171, 2014.

[13] J. Steckel and H. Peremans, "Ultrasound-based Air Leak Detection using a Random Microphone Array and Sparse Representations," presented at the IEEE Sensors Conference, Valencia, Spain, Nov. 2014.

[14] T. Guo, T. Zhang, E. Lim, M. López-Benítez, F. Ma, and L. Yu, "A Review of Wavelet Analysis and Its Applications: Challenges and Opportunities," IEEE Access, vol. 10, pp. 3179517, 2022.

[15] T. Stratoudaki, M. Clark, and P. D. Wilcox, "Laser induced ultrasonic phased array using full matrix capture data acquisition and total focusing method," presented at the IEEE Sensors Conference, Valencia, Spain, Nov. 2014.

[16] M. Mirzaei, A. Asif, and H. Rivaz, "Virtual Source Synthetic Aperture for Accurate Lateral Displacement Estimation in Ultrasound Elastography," arXiv, vol. 10, no. 2, pp. 1–9, 2020. doi:10.48550/arXiv.2012.10562.

[17] K. Sreekala and E. Krishna Kumar, "Compressed Sensing in Imaging and Reconstruction - An Insight Review," in Intelligent Systems Design and Applications, Springer, 2019, pp. 779–791.

[18] Senscomp. Series 7000 Ultrasonic Sensor Datasheet. (734):1–3, 2014.

[19] Jan Steckel, Andre Boen, and Herbert Peremans, "Broadband 3-D sonar system using a sparse array for indoor navigation, " IEEE Transactions on Robotics, 29(1):161–171, 2013.

[20] Robin Kerstens, Dennis Laurijssen, and Jan Steckel, " Low-cost One-bit MEMS Microphone Arrays for In-air Acoustic Imaging Using FPGA's, " In IEEE SENSORS, pages 1–3, Glasgow, 2017.

[21] H L Van Trees, "Optimum Array Processing: Part IV of Detection, Estimation, and Modulation Theory. Detection, Estimation, and Modulation Theory, " Wiley, 2004.

[22] J. Steckel and H. Peremans, "Sparse decomposition of in-air sonar images for object localization, " IEEE SENSORS 2014 Proceedings, (1):1356–1359, 2014.

[23] Jan Steckel, Andre Boen, and Herbert Peremans, "Broadband 3-D sonar system using a sparse array for indoor navigation," IEEE Transactions on Robotics, 29(1):161–171, 2013.

[24] I. Djurek, T. Grubeša, and I. Križanić,"Measurements and Evaluation of a PDM Output Digital MEMS Microphone," Scientific Society for Optics, Acoustics, Motion Pictures and Theatre, 2021.

[25] E. Por, M. van Kooten, and V. Sarkovic, "Nyquist–Shannon sampling theorem," May 2019.

[26] M.Manesh, N.Kaabouch, and H. Reyes, "A Comparative Study of Spectrum Sensing Techniques for Cognitive Radio Systems," IEEE.

[27] E. J. Candès and M. B. Wakin, "An introduction to compressive sampling," IEEE signal processing magazine, Vols. 25(2), pp. 21-30, 2008.

[28] J. Dai, A. Liu, and H. C. So, "Sparse Bayesian Learning Approach for Discrete Signal Reconstruction," arXiv:1906.00309v1, 2019.